

Total Synthesis of Tetrodotoxin and 9-*epi*Tetrodotoxin

Authors: Peihao Chen^{1,3†}, Jing Wang^{2,3,4†}, Yan Wang^{2,3,4}, Yuze Sun³, Songlin Bai^{2,3,4}, Qingcui Wu³, Shuangfeng Zhang³, Xinyu Cheng^{3,5}, Peng Cao^{3,4}, Xiangbing Qi^{3,4*}

Affiliations:

¹School of Life Sciences, Peking University, Beijing 100871, China.

²School of Life Sciences, Tsinghua University, Beijing 100084, China.

³National Institute of Biological Sciences, 7 Science Park Road, Zhongguancun Life Science Park, Beijing 102206, China.

⁴Tsinghua Institute of Multidisciplinary Biomedical Research, Tsinghua University, Beijing 100084, China.

⁵National Institute of Biological Sciences, Chinese Academy of Medical Sciences&Peking Union Medical College, Beijing 100730, China.

† These authors contributed equally to this work.

* Corresponding author. Email: qixiangbing@nibs.ac.cn (X. Q.)

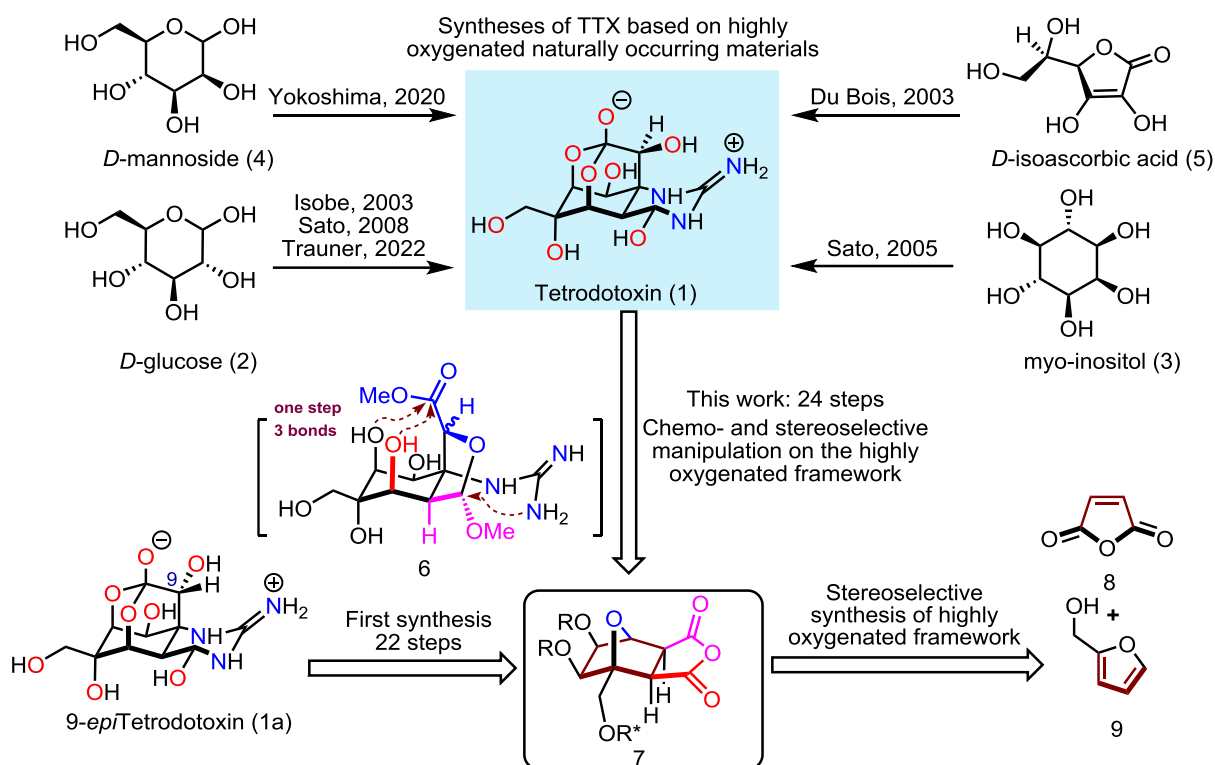
Abstract:

Tetrodotoxin and congeners are specific voltage-gated sodium channel blockers that exhibit remarkable anesthetic and analgesic effects. Here, we present a scalable asymmetric synthesis of TTX and 9-*epi*TTX from the abundant chemical feedstock furfuryl alcohol. The optically pure cyclohexane skeleton was assembled via a stereoselective Diels-Alder reaction. The dense heteroatom substituents were established sequentially by a series of functional group interconversions on highly oxygenated cyclohexane frameworks, including a chemoselective cyclic anhydride opening, and a decarboxylative hydroxylation. An innovative SmI₂-mediated concurrent fragmentation, an oxo-bridge ring opening and ester reduction followed by an Upjohn dihydroxylation delivered the highly oxidized skeleton. Ruthenium-catalyzed oxidative alkyne cleavage and formation of the hemiaminal and orthoester under acidic conditions enabled the rapid assembly of TTX, anhydro-TTX, 9-*epi*TTX, and 9-*epi* lactone-TTX.

Main text:

32 Tetrodotoxin (TTX, **1**), is one of the most potent neurotoxins with a complex structure, and
33 analgesic effects. After the first isolation of TTX in 1909,¹ the structure of this highly polar
34 zwitterion was solved by Woodward,^{2,3} Tsuda,⁴ Goto,⁵ and Mosher⁶ simultaneously in 1964 using
35 degradative methods and NMR spectroscopy. TTX's unique structure comprises a densely heteroatom-
36 substituted, stereochemically complex framework that has a rigid dioxo-adamantane cage with an ortho
37 acid, a cyclic guanidinium hemiaminal moiety, and nine contiguous stereogenic centers, including one
38 bridgehead nitrogen-containing quaternary center. There are three compounds in equilibrium—ortho
39 ester, 4,9-anhydro, and lactone, that are known to interconvert under acidic conditions.^{7,8} Recently, the
40 TTX analogue 9-*epi*Tetrodotoxin (**1a**, **Figure 1**) was isolated as an equilibrium mixture of the
41 hemilactal and 10,8-lactone forms.⁹ TTX is neurotoxic and exhibits prominent anesthetic and
42 analgesic properties in animal models. The mode of action of this bipolar molecule is defined by its
43 disruption of voltage-gated sodium ion channels (Na_v), which was originally suggested in the early
44 1960s,^{10,11} and was recently confirmed by crystallographic studies.^{12,13} Extensive pharmacological
45 investigations, including clinical trials,¹⁴ have demonstrated the immense promise of TTX in pain
46 treatment and detoxification from heroin addiction; accordingly, a reliable source of TTX is of
47 practical significance.

48 The remarkably polar functionality, stereochemically complex architecture, and fascinating
49 biological activity, have made this compound an attractive synthetic target. To date, numerous efforts
50 have been made towards the total synthesis of TTX, with the first synthesis by Kishi in 1972.^{15,16}
51 Subsequently, asymmetric syntheses have been achieved by Isobe,^{8,17} Du Bois,¹⁸ Sato,¹⁹⁻²¹
52 Fukuyama,²² Yokoshima,²³ and Marin.²⁴ More recently, Trauner described an elegant and concise
53 asymmetric synthesis of TTX based on a glucose derivative.²⁵ In addition to these syntheses, TTX has



54 **Fig. 1| Previous syntheses of Tetrodotoxin and retrosynthetic analysis.**

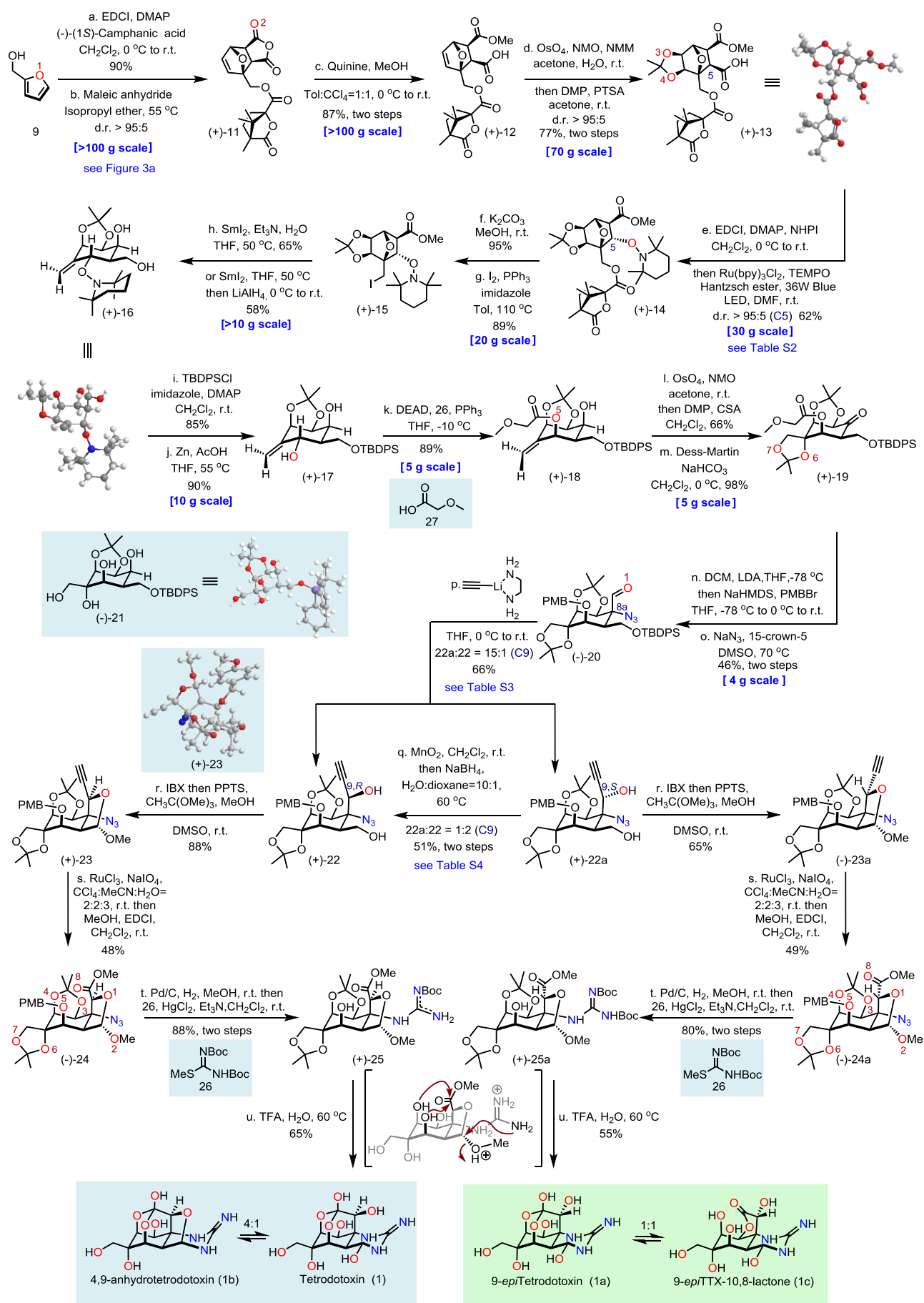
55 also been a model compound for demonstrating creative synthetic strategies, in assembling this type
 56 of highly oxygenated guanidinium alkaloids efficiently (Keana,²⁶⁻²⁸ Burgey,²⁹ Alonso,³⁰⁻³³ Taber,³⁴
 57 Shinada,³⁵ Ciufolini,^{36,37} Hudlicky,³⁸ Nishikawa³⁹⁻⁴² and Johnson^{43,44}).

58 Precise functional group manipulations on heavily heteroatom-substituted, stereochemically
 59 complex frameworks have proven challenging, as evidenced by the total synthesis of highly oxidized
 60 natural products,⁴⁵⁻⁵³ and as exemplified by the synthetic studies of TTX by Isobe,⁸ Du Bios,¹⁸
 61 Sato,^{19,20} Yokoshima,²³ and Trauner²⁵(**Figure 1**) using highly oxygenated natural starting materials
 62 such as, *D*-glucose (2), myo-inositol (3), *D*-mannoside (4), or *D*-isoascorbic acid (5). Although the
 63 preexisting oxygen functionality in these naturally occurring materials provides the functionality basis
 64 of TTX, efficient and precise interconversion of these similar functionalities on the densely
 65 heteroatom-substituted skeleton in a chemo and stereoselective manner is arduous. We envisioned that
 66 if the highly oxygenated framework could be assembled rapidly in the early stage in a stereo-

67 controllable fashion and followed by sequential chemo and stereoselective functional group
68 manipulations might provide a practical solution to a concise synthesis of TTX and its congeners
69 (**Figure 1**). Here, we describe a distinct synthetic strategy that streamlines the incorporation of the
70 dense heteroatom-substituted architecture and is amenable to a scalable synthesis of 9-*epi*TTX and
71 TTX (>15 mg, which is the largest scale known in literature).

72 Retrosynthetic analysis (**Figure 1**) reveals that the hemiaminal and orthoester moieties of the
73 complex dioxo-adamantane architecture can be obtained in one step from intermediate **6**, in which both
74 the ester and guanidinium groups are built upon the bridgehead oxygen functionality of framework **7**
75 via a series of well-planned events: SmI₂-mediated reductive oxo-bridge ring opening, Dess-Martin
76 oxidation, chloroepoxidation,^{20,54,55} stereoselective epoxide opening, and ruthenium-catalyzed
77 oxidative alkyne cleavage. The anhydride motif of **7** is initially transformed into chemically
78 differentiated mono-acid and mono-ester by regioselective methanolysis, which lays the foundation
79 for subsequent radical decarboxylative hydroxylation and hemiaminal synthesis from the redox
80 manipulation of the ester. To access the highly oxygenated chiral framework **7**, a stereoselective
81 strategy is proposed from a chiral auxiliary assisted Diels-Alder reaction of the easily accessible maleic
82 anhydride **8** and furfuryl alcohol **9**.

83 The synthesis of TTX (**1**) was initiated with the stereoselective construction of the oxygen-
84 substituted cyclohexane skeleton (**Figure 2**). The first oxygen functionality was derived from furfuryl
85 alcohol **9** directly. Esterification of furfuryl alcohol **9** with chiral auxiliary (-)-(1*S*)-camphanic acid
86 afforded ester **10**. To achieve the enantiomerically pure 7-oxabicyclo[2.2.1]hept-2-ene derivative **11**,⁵⁶
87 we developed a reliable stereoselective Diels-Alder protocol by heating **10** with maleic anhydride in
88 the presence of isopropyl ether as the solvent (see **Figure 3a and Table S1**). Initially, the original pro-

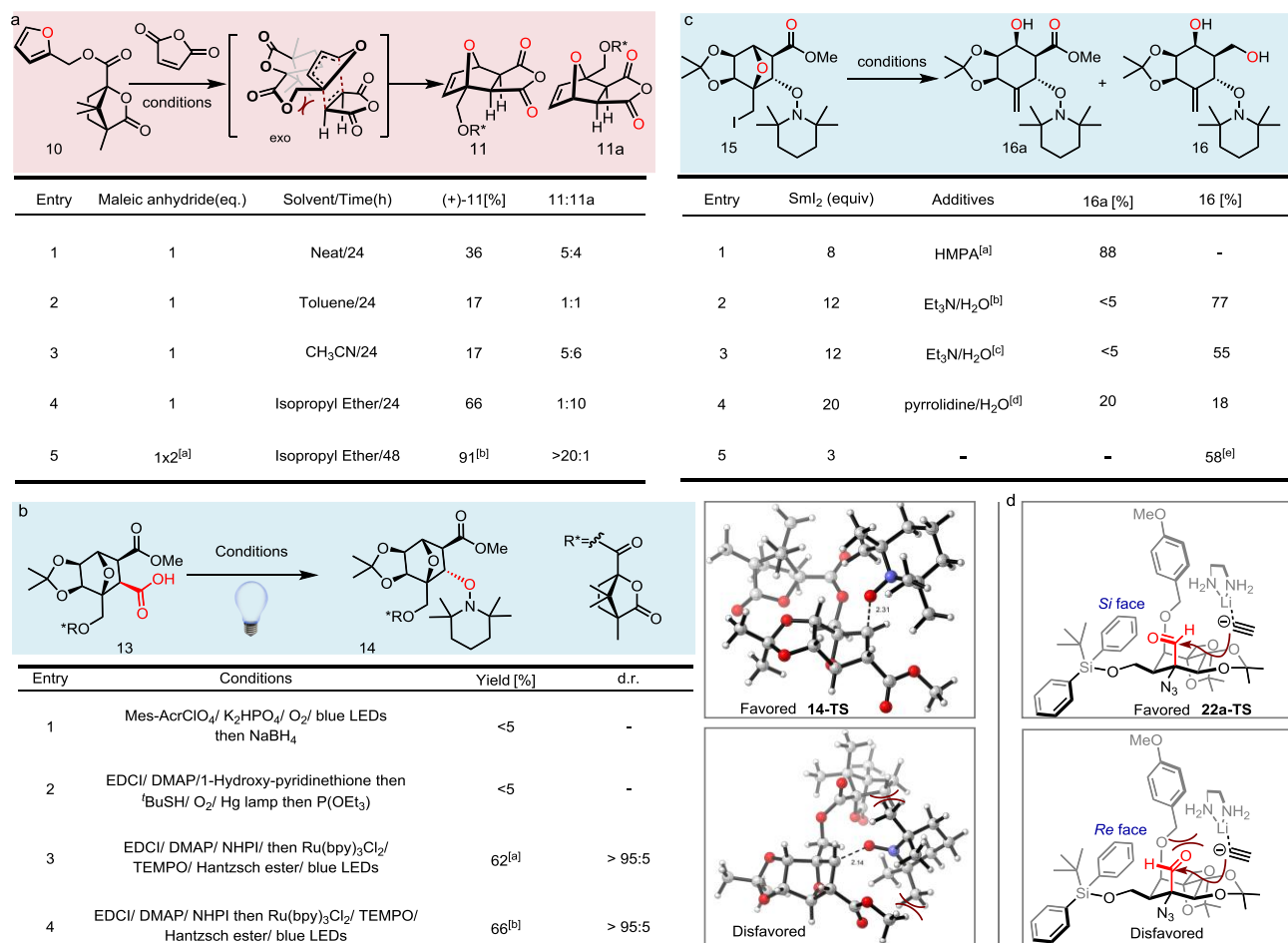


89 Fig. 2| Completion of total synthesis of TTX and 9-*epi*TTX.

90 tocol by Vogel⁵⁶ under neat conditions was attempted, but only a 5:4 mixture of two inseparable *exo*
91 adducts **11** and **11a** was observed (by ¹H-NMR analysis of the reaction mixture). Investigation of
92 reaction conditions including the effects of molar ratio of reactants, Lewis acids, reaction time, and the
93 temperature was unfruitful in terms of either yield or diastereoselectivity.

94 Consequently, a survey of solvents was conducted and the use of isopropyl ether was found to be
95 the crucial factor for the successful generation of optically pure diastereomer **11** as a single detectable
96 *exo* cycloadduct (**ratio of 11: 11a >20:1**). The high *exo*-selectivity observed in the current
97 cycloaddition is presumably resulted from the retro-Diels–Alder fragmentation of unstable *endo*
98 cycloadduct.⁵⁷ However, whether the chiral auxiliary (-)-(1*S*)-camphanic acid plays a stereoselective
99 control for Diels–Alder cycloaddition or promotes the crystallization-based enrichment is still a puzzle
100 since no other diastereomers were detected during the whole process, which is inconsistent with the
101 observation by Vogel⁵⁶. This stereoselective cycloaddition established the second oxygen functionality
102 and could be scaled up to 100 grams without erosion of yield or stereoselectivity. Quinine-mediated
103 regioselective methanolysis⁵⁸ of anhydride **11** resulted in the methyl ester and acid **12**. Subsequently,
104 a stereospecific Upjohn *exo*-dihydroxylation⁵⁹ of the olefin established the third and the fourth oxygen
105 functionalities (with simultaneous 1,2-diol protection) and produced the mono-acid **13**, whose
106 structure was confirmed by X-ray crystallographic analysis of the single crystal (CCDC#: 2184304).

107 Decarboxylative hydroxylation was carried out to introduce the fifth oxygen functionality at the
108 C5 position. Initially, high-valent metal reagents were examined as oxidants but were inadequate
109 owing to substrate decomposition. Mild radical conditions, including Barton or organophotoredox-
110 promoted decarboxylation in the presence of a radical initiator and oxygen under UV irradiation,⁶⁰⁻⁶²
111 were also unsuccessful (see **Figure 3b**). After considerable experimentation, a Ru-catalyzed photore-



112

113 **Fig. 3| Optimization of reaction conditions.** The yields were determined by ¹H NMR with 1,3,5-
 114 trimethoxybenzene as the internal standard. **a**, Optimization of the Diels-Alder reaction. [a] After 12h, the same
 115 eq maleic anhydride was added. [b] Scale up to 100 grams, isolated yield with 6% (molar ratio) maleic anhydride.
 116 **b**, Optimization of decarboxylative hydroxylation. [a] d.r. > 95:5, 30 g scale. [b] Isolated yield on 1 g scale
 117 using a circulating flow system, 24h. **c**, Optimization of the SmI₂/H₂O/amine-mediated fragmentation. [a]
 118 HMPA (10 eq). [b] Et₃N (24 eq)/H₂O (24 eq). [c] Et₃N (36 eq)/H₂O (36 eq). [d] pyrrolidine (60 eq)/H₂O (60
 119 eq). [e] SmI₂ (3 eq), 55 °C, without purification followed by reduction using LiAlH₄. Isolated yields for the two
 120 steps on decagram scale. **d**, Selectivity of nucleophilic addition. *N.D., not determined. *NHPI: N-
 121 Hydroxyphthalimide, *MTBE: methyl tert-butyl ether.

122 dox decarboxylative hydroxylation⁶³ of the *N*-hydroxyphthalimide (NHPI) ester of **13** as
 123 a single detectable diastereomer in 66% yield, albeit with an inverted configuration at C5 relative to
 124 TTX. Previous syntheses^{8,18} revealed that steric hindrance at the C5 position is troublesome for the
 125 following functional group manipulations. Therefore, we utilized a late-stage configurational inversion
 126 strategy to simplify the stereoselective oxygen functionality installation sequence. Notably, this
 127 photoredox decarboxylative hydroxylation could also be scaled up by employing circulating flow

128 photochemistry without compromising the yields or diastereoselectivity (**entry 4, Figure 3b**). To
129 interpret the diastereoselectivity and analyze the steric effect of this radical addition, we performed the
130 density functional theory (DFT) calculations. The DFT calculations support a clear radical addition
131 preference for the experimentally observed stereoisomer at C5 that stems from the radical addition
132 from the convex face of the oxo-bridge ring. ($\Delta\Delta G=3.4$ kcal/mol and predicted dr > 99:1, details of
133 computation results are shown in the supplementary information.)

134 With compound **14** in hand, we investigated the functional group interconversions of this oxo-
135 bridge ring system and developed a reaction sequence to build the oxygen functionalities at the C8a,
136 C6, and C11 positions. The auxiliary (-)-camphanic acid was first removed by transesterification with
137 methanol, providing the primary alcohol, which was then subjected to an Appel reaction giving the
138 alkyl iodide **15**. The chiral auxiliary could be recycled as methyl camphanate. A variety of reductive
139 conditions applied to the alkyl iodide **15** failed to produce the desired oxo-bridge ring-opening product.
140 After intensive exploration of the reductive conditions, we developed a successful reaction sequence
141 (**Figure 3c**): the initial SmI₂ mediated single electron transfer homolytically cleaved the carbon-iodide
142 bond and generated a primary carbon radical, which could be further reduced by Sm(II) to a
143 carbanion^{64,65} to drive the bridged C-O bond cleavage. The primary alcohol was generated from
144 concurrent methyl ester reduction by SmI₂, while the N-O bond of TEMPO remained unaffected due
145 to steric hindrance. In the presence of hexamethylphosphoramide (HMPA), only intermediate **16a** was
146 obtained without reduction of the methyl ester to diol **16** (**entry 1, Figure 3c**). Activation of SmI₂ with
147 H₂O and Et₃N in a 1:2:2 ratio created a stronger reductant,⁶⁶ which allowed for the reduction of the
148 methyl ester (**entry 2**) in a 77% yield as determined by ¹H NMR. Increasing amounts of H₂O and Et₃N
149 or replacing Et₃N with pyrrolidine resulted in complex product mixtures (**entries 3 and 4**). The

150 procedure could also be modified to a two-step protocol involving fewer equivalents of SmI₂ to afford
151 **16a**, followed by a LiAlH₄ reduction to give **16** in 58% yield on a decagram scale (**entry 5**). The
152 relative configuration of **16** was verified by X-ray crystallography of the single crystal (CCDC#:
153 2182018).

154 The construction of azidoaldehyde **20** started with selective protection of the primary alcohol in
155 **16** using the sterically hindered TBDPSCl. The N-O bond of TEMPO in the resulting alkene was
156 reductively cleaved with Zn powder giving the allylic alcohol **17**. The incorrect configuration of C5-
157 OH was then inverted by a chemoselective Mitsunobu reaction of C5 allylic alcohol in the presence of
158 free C8a secondary alcohol with 2-methoxyacetic acid **27**, delivering the fifth oxygen functionality in
159 **18** in excellent yield. Other acids such as acetic acid or benzyloxyacetic acid afforded products in low
160 yields. The sixth and seventh oxygen functionalities were established via a diastereoselective Upjohn
161 dihydroxylation followed by protection as the acetonide, whose relative configuration was confirmed
162 by X-ray crystallography of the derivative **21** (CCDC#: 2184298) (See the supplementary information).
163 The secondary alcohol underwent Dess-Martin oxidation to afford the ketone **19** in excellent yield. An
164 intramolecular Mannich reaction between the α position of methoxyacetic acid and the ketone **19**
165 derived imine was unfeasible. The intermolecular nucleophilic addition of a variety of nucleophiles
166 also exclusively produced a diastereomer with the wrong configuration at C8a (See **Scheme S2**).
167 Although Darzens reaction of **19** with α -haloester smoothly generated an α, β -epoxy ester (glycidic
168 ester), the stereoselective and regioselective epoxide opening strategy proved unfruitful in the presence
169 of different types of nitrogen-based nucleophiles (**Scheme S2**). The nucleophilic addition of Sato's
170 dichloromethylithium (LiCHCl₂) to the ketone **19** was successfully afforded the spiro α -
171 chloroepoxide as a single diastereomer^{20,54} and concurrently removed the ester group at C5-OH, which

172 was protected with a *p*-methoxybenzyl group (PMB) in one pot. Regioselective epoxide opening of
173 the resulting chloroepoxide with NaN₃ proceeded smoothly to afford the α -azido aldehyde **20** on a
174 gram-scale, with the correct configuration of the C8a quaternary stereogenic center.

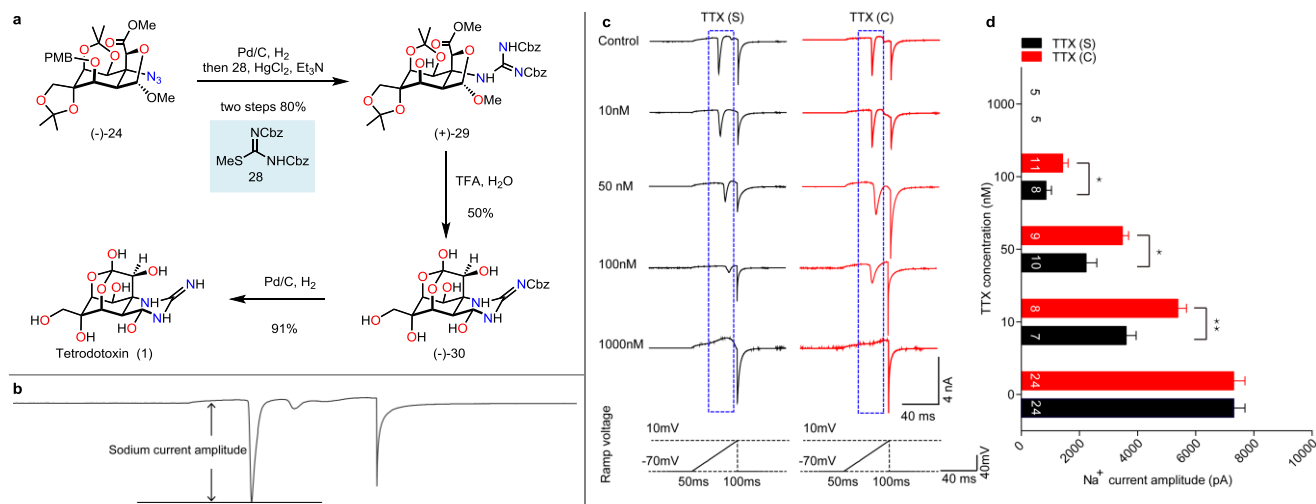
175 With the construction of the highly oxygen-substituted carbocyclic core **20** accomplished, we
176 began to address the synthetic challenge of constructing the complex dioxo-adamantane core and the
177 guanidinium hemiaminal moieties. The α -azido aldehyde **20** was subjected to a 1,2-addition with
178 lithium acetylide (**Table S2**), followed by the removal of the TBDPS group to produce two
179 diastereomers (**22/22a**=1:15) that could undergo divergent synthesis to both TTX and *9-epi*TTX.
180 Presumably owing to the steric hindrance introduced by the bulky TBDPS and PMB groups, the
181 lithium acetylide preferentially attacked from the less sterically hindered *si* face and generated the
182 undesired diastereomer **22a** (**Figure 3d**). Extensive exploration of the reaction conditions revealed that
183 the stereochemistry of C9 of **22a** could be inverted in a 2:1 ratio (**22/22a**=2:1) via sequential MnO₂-
184 mediated chemoselective oxidation followed by NaBH₄ reduction (**Table S3**). IBX oxidation of the
185 primary alcohol **22** provided the corresponding bridged hemiacetal, which was converted to the acetal
186 **23** with trimethylorthoacetate. The structure and the stereochemistry of **23** were confirmed by single-
187 crystal X-ray crystallography (CCDC#: 2184305). Distinct from previous syntheses that heavily
188 focused on the lactone formation between C5-OH and the C10-COOH as the advanced intermediate,
189 our strategy pinpointed the issue of conformational control for precise functional group manipulations
190 on the stereochemically complex framework. Decreasing the conformational flexibility by the bridged
191 tetrahydrofuran acetal ring formed between C9 and C4 is critical to the efficiency of the following
192 transformations including alkyne oxidative cleavage, guanidine installation, and one-step cyclic

193 guanidinium hemiaminal and orthoester formation, thus demonstrating a unique and concise strategy
194 for the final stage of TTX synthesis.

195 Oxidative cleavage of alkyne **23** with RuCl₃/NaIO₄ followed by esterification afforded methyl
196 carboxylate **24**. Simultaneous PMB deprotection and azido reduction by hydrogenation efficiently
197 delivered the tertiary amine, which was guanidinylated⁶⁷ *in situ* with bis-Boc protected isothioureia **26**,
198 leading to the penultimate intermediate **25**. To our delight, treatment of this unprecedented compound
199 **25** with trifluoroacetic acid at 60 °C afforded a global deprotection and successfully installed both the
200 hemiaminal and the orthoester of TTX, leading to the final product TTX (**1**) and 4,9-anhydroTTX (**1b**)
201 in a 1:1 mixture. The use of 2% TFA-*d* in deuterium oxide further converted this mixture to a 4:1 ratio
202 favoring TTX (see supplementary information).⁸ A similar synthetic process was used to convert the
203 diastereomer **22a** to the final 9-*epi*TTX (**1a**) and its 10,8-lactone form (**1c**) in 5 steps (14% overall
204 yields). The spectroscopic data (¹H NMR, ¹³C NMR, HRMS) of synthetic TTX and 9-*epi*TTX were
205 identical to those of the authentic reference samples^{7,8}.

206 TTX in most biomedical studies is a mixture in equilibrium with the ortho ester, the lactone form,
207 and 4,9-anhydroTTX.^{8,11} To investigate the biological activities of a pure TTX, we synthesized and
208 purified a single form of TTX (**S**) from the methyl carboxylate **24** (**Figure 4a**) according to
209 Fukuyama's strategy.²² A commercial sample named TTX (**C**) (the ratio of TTX to 4,9-anhydroTTX
210 was 3:1 as analyzed by ¹H NMR, **Figure S1**) was utilized for comparison. In mice, primary
211 hippocampal neurons cultured for 14 days displayed a mature sodium current property (**Figure 4b**).
212 Both samples at 1 μM concentration were sufficient to block sodium currents in cultured hippocampal
213 neurons (**Figure 4c**). Next, we detected the Na_v blocking effects of these two TTX samples across a
214 range of concentrations (10 nM, 50 nM, 100 nM). Compared to TTX (**C**), our synthetic pure TTX (**S**)

215 showed a stronger effect in decreasing the sodium current amplitude in wild-type div (days *in vitro*)
 216 14 hippocampal neurons (**Figure 4d**).



217 **Fig. 4| Alternative synthesis of pure TTX and effects of TTX (Synthetic) and TTX (Commercial) on**
 218 **depolarization-induced sodium currents.** **a**, The procedure of preparing high purity TTX. **b**, Schematic
 219 diagram for sodium current evoked by a ramp voltage. **c**, Representative traces for sodium current amplitudes
 220 in primary cultured hippocampal neurons (DIV14) after treatment with various TTX compounds. Black, TTX
 221 (Synthetic); Red, TTX (Commercial). Ramp voltage from -70 mV to 10 mV over 50-ms. **d**, Quantitative
 222 analyses of sodium current amplitude in neurons treated with TTX (Synthetic) and TTX (Commercial)
 223 with various concentrations. Cell numbers are marked on the columns. Error bars represent means \pm SEM; two-tailed
 224 unpaired t-test, *P < 0.05, **P < 0.01.

225

226 In summary, we have achieved the first asymmetric synthesis of 9-*epi*TTX (**1a**) (22 steps) and
 227 one of the shortest syntheses of TTX (**1**) (24 steps, following the Rules for Calculating Step Counts^{68,69})
 228 from the easily accessible furfuryl alcohol. The hundred-gram-scale asymmetric preparation of
 229 cyclohexane (+)-**12** showcases the power of the stereoselective Diels-Alder reaction in the scale-up
 230 synthesis of a carbocyclic ring with a dense array of functionalities.⁷⁰ The precise introduction of the
 231 oxygen functionality at the C-5 position via photochemical decarboxylative hydroxylation highlights
 232 the advance of free radical transformation performed on a sterically demanding carbocyclic skeleton.
 233 The SmI₂-mediated sequential reactions of reductive fragmentation, oxo-bridge ring opening, and ester
 234 reduction, followed by diastereoselective Upjohn dihydroxylation enable a gram-scale synthesis of

235 highly oxidized intermediate (+)-**19**. The bridged tetrahydrofuran acetal setting simplifies the endgame
236 and facilitates the rapid formation of the cyclic guanidinium hemiaminal and orthoester in one pot.
237 Notably, the present synthesis served as a testbed for precise functional group manipulations on the
238 densely functionalized and stereochemically complex frameworks and should be readily applicable to
239 the synthesis of other heavily oxygenated polycyclic natural products. The concise synthetic strategy
240 is suitable for the production of TTX congeners or derivatives that support further pharmacology
241 investigations and should be amenable to large-scale synthesis of TTX for analgesic drug development,
242 particularly for non-opioid cancer pain treatment.

243

244 **References:**

- 245 1 Tahara, Y. & Hirata, Y. Studies on the puffer fish toxin. *J. Pharm.Soc.Jpn.* **29**, 587-625 (1909).
- 246 2 Woodward, R. B. The structure of tetrodotoxin. *Pure and Applied Chemistry* **9**, 49-74 (1964).
- 247 3 Woodward, R. B. & Gougoutas, J. Z. The Structure of Tetrodotoxin. *J. Am. Chem. Soc.* **86**,
248 5030-5030 (1964).
- 249 4 Tsuda, K. *et al.* On the constitution and configuration of anhydrotetrodotoxin. *Chem. Pharm.*
250 *Bull.* **12**, 634-642 (1964).
- 251 5 Goto, T., Kishi, Y., Takahashi, S. & Hirata, Y. Tetrodotoxin. *Tetrahedron* **21**, 2059-2088 (1965).
- 252 6 Mosher, H. S., Fuhrman, F. A., Buchwald, H. D. & Fischer, H. G. Tarichatoxin—Tetrodotoxin:
253 a potent neurotoxin. *Science* **144**, 1100-1110 (1964).
- 254 7 Yasumoto, T., Yotsu, M., Murata, M. & Naoki, H. New tetrodotoxin analogs from the newt
255 *Cynops ensicauda*. *J. Am. Chem. Soc.* **110**, 2344-2345 (1988).
- 256 8 Ohyabu, N., Nishikawa, T. & Isobe, M. First Asymmetric Total Synthesis of Tetrodotoxin. *J.*
257 *Am. Chem. Soc.* **125**, 8798-8805 (2003).
- 258 9 Yaegashi, Y. *et al.* Isolation and Biological Activity of 9-*epi*Tetrodotoxin and Isolation of Tb-
259 242B, Possible Biosynthetic Shunt Products of Tetrodotoxin from Pufferfish. *J. Nat. Prod.* **85**,
260 2199-2206 (2022).
- 261 10 Narahashi, T., Moore, J. W. & Scott, W. R. Tetrodotoxin blockage of sodium conductance
262 increase in lobster giant axons. *J. Gen. Physiol.* **47**, 965-974 (1964).
- 263 11 Makarova, M., Rycek, L., Hajicek, J., Baidilov, D. & Hudlicky, T. Tetrodotoxin: History,
264 Biology, and Synthesis. *Angew. Chem., Int. Ed.* **58**, 18338-18387 (2019).
- 265 12 Shen, H. *et al.* Structural basis for the modulation of voltage-gated sodium channels by animal
266 toxins. *Science* **362**, eaau2596 (2018).
- 267 13 Shen, H., Liu, D., Wu, K., Lei, J. & Yan, N. Structures of human Nav1.7 channel in complex
268 with auxiliary subunits and animal toxins. *Science* **363**, 1303-1308 (2019).
- 269 14 Hagen, N. A. *et al.* Tetrodotoxin for Moderate to Severe Cancer-Related Pain: A Multicentre,
270 Randomized, Double-Blind, Placebo-Controlled, Parallel-Design Trial. *Pain research &*

- 271 *management* **2017**, 7212713 (2017).
- 272 15 Kishi, Y., Aratani, M., Fukuyama, T., Nakatsubo, F. & Goto, T. Synthetic studies on
273 tetrodotoxin and related compounds. 3. A stereospecific synthesis of an equivalent of acetylated
274 tetrodamine. *J. Am. Chem. Soc.* **94**, 9217-9219 (1972).
- 275 16 Kishi, Y. *et al.* Synthetic studies on tetrodotoxin and related compounds. IV. Stereospecific total
276 syntheses of *DL*-tetrodotoxin. *J. Am. Chem. Soc.* **94**, 9219-9221 (1972).
- 277 17 Nishikawa, T., Urabe, D. & Isobe, M. An efficient total synthesis of optically active
278 tetrodotoxin. *Angew. Chem., Int. Ed.* **43**, 4782-4785 (2004).
- 279 18 Hinman, A. & Du Bois, J. A stereoselective synthesis of (–)-tetrodotoxin. *J. Am. Chem. Soc.*
280 **125**, 11510-11511 (2003).
- 281 19 Sato, K.-i. *et al.* Novel and Stereocontrolled Synthesis of (±)-Tetrodotoxin from myo-Inositol.
282 *J. Org. Chem.* **70**, 7496-7504 (2005).
- 283 20 Sato, K.-i. *et al.* Stereoselective and efficient total synthesis of optically active tetrodotoxin
284 from D-glucose. *J. Org. Chem.* **73**, 1234-1242 (2008).
- 285 21 Akai, S. *et al.* Total Synthesis of (–)-Tetrodotoxin from D-Glucose: A New Route to Multi-
286 Functionalized Cyclitol Employing the Ferrier(II) Reaction toward (–)-Tetrodotoxin. *Bulletin*
287 *of the Chemical Society of Japan* **83**, 279-287 (2010).
- 288 22 Maehara, T., Motoyama, K., Toma, T., Yokoshima, S. & Fukuyama, T. Total Synthesis of (–)-
289 Tetrodotoxin and 11-norTTX-6(*R*)-ol. *Angew. Chem. Int. Ed.* **56**, 1549-1552 (2017).
- 290 23 Murakami, K., Toma, T., Fukuyama, T. & Yokoshima, S. Total Synthesis of Tetrodotoxin.
291 *Angew. Chem. Int. Ed.* **59**, 6253-6257 (2020).
- 292 24 P. N. Marin (Esteve Pharmaceuticals SA), EP1785427A1. (2007).
- 293 25 Konrad, D. B. *et al.* A concise synthesis of tetrodotoxin. *Science* **377**, 411-415 (2022).
- 294 26 Keana, J. F. W., Mason, F. P. & Bland, J. S. Synthetic intermediates potentially useful for the
295 synthesis of tetrodotoxin and derivatives. *J. Org. Chem.* **34**, 3705-3707 (1969).
- 296 27 Keana, J. F. W. & Kim, C. U. Synthetic intermediates potentially useful for the synthesis of
297 tetrodotoxin and derivatives. II. Reaction of diazomethane with some shikimic acid derivatives.
298 *J. Org. Chem.* **35**, 1093-1096 (1970).
- 299 28 Keana, J. F. W. & Kim, C. U. Synthetic intermediates potentially useful for the synthesis of
300 tetrodotoxin and derivatives. III. Synthesis of a key lactone intermediate from shikimic acid. *J.*
301 *Org. Chem.* **36**, 118-127 (1971).
- 302 29 Burgey, C. S., Vollerthun, R. & Fraser-Reid, B. Armed/Disarmed Effects and Adamantyl
303 Expansion of Some Caged Tricyclic Acetals en Route to Tetrodotoxin_{1,2}. *J. Org. Chem.* **61**,
304 1609-1618 (1996).
- 305 30 Noya, B. & Alonso, R. Radical cyclisation onto C-3 of 1, 6-anhydro-β-d-mannopyranose
306 derivatives. Application to the formation of the C8a centre of (–)-tetrodotoxin. *Tetrahedron*
307 *Letters* **38**, 2745-2748 (1997).
- 308 31 Noya, B., Paredes, M. D., Ozores, L. & Alonso, R. 5-exo Radical Cyclization onto 3-
309 Alkoxyketimino-1,6-anhydromannopyranoses. Efficient Preparation of Synthetic
310 Intermediates for (–)-Tetrodotoxin. *J. Org. Chem.* **65**, 5960-5968 (2000).
- 311 32 Cagide - Fagín, F. & Alonso, R. A cascade annulation based convergent approach to racemic
312 tetrodotoxin. *Eur. J. Org. Chem.* **35**, 6741-6747 (2010).
- 313 33 Lago-Santomé, H., Meana-Pañeda, R. & Alonso, R. A Convergent Approach to the
314 Dioxadamantane Core of (±)-Tetrodotoxin. *J. Org. Chem.* **79**, 4300-4305 (2014).

- 315 34 Taber, D. F. & Storck, P. H. Synthesis of (–)-Tetrodotoxin: Preparation of an Advanced
316 Cyclohexenone Intermediate. *J. Org. Chem.* **68**, 7768-7771 (2003).
- 317 35 Manabe, A., Ohfuné, Y. & Shinada, T. Toward the total synthesis of tetrodotoxin:
318 stereoselective construction of the 7-oxanorbornane intermediate. *Tetrahedron Letters* **55**,
319 6077-6080 (2014).
- 320 36 Mendelsohn, B. A. & Ciufolini, M. A. Approach to tetrodotoxin via the oxidative amidation of
321 a phenol. *Org. Lett.* **11**, 4736-4739 (2009).
- 322 37 Chau, J., Xu, S. & Ciufolini, M. A. Assembly of a Key Dienic Intermediate for Tetrodotoxin
323 via a Machetti–DeSarlo Reaction. *J. Org. Chem.* **78**, 11901-11910 (2013).
- 324 38 Baidilov, D. *et al.* Chemoenzymatic synthesis of advanced intermediates for formal total
325 syntheses of tetrodotoxin. *Angew. Chem., Int. Ed.* **130**, 11160-11164 (2018).
- 326 39 Adachi, M. *et al.* Total Syntheses and Determination of Absolute Configurations of Cep-212
327 and Cep-210, Predicted Biosynthetic Intermediates of Tetrodotoxin Isolated from Toxic Newt.
328 *Org. Lett.* **21**, 780-784 (2019).
- 329 40 Miyasaka, T., Adachi, M. & Nishikawa, T. Synthesis of the 8-Deoxy Analogue of 4,9-Anhydro-
330 10-hemiketal-5-deoxy-tetrodotoxin, a Proposed Biosynthetic Precursor of Tetrodotoxin. *Org.*
331 *Lett.* **23**, 9232-9236 (2021).
- 332 41 Nishikawa, K. *et al.* Tetrodotoxin Framework Construction from Linear Substrates Utilizing a
333 Hg(OTf)₂-Catalyzed Cycloisomerization Reaction: Synthesis of the Unnatural Analogue 11-
334 nor-6,7,8-Trideoxytetrodotoxin. *Org. Lett.* **23**, 1703-1708 (2021).
- 335 42 Nishiumi, M., Miyasaka, T., Adachi, M. & Nishikawa, T. Total Syntheses of the Proposed
336 Biosynthetic Intermediates of Tetrodotoxin Tb-210B, Tb-226, Tb-242C, and Tb-258. *J. Org.*
337 *Chem.* **87**, 9023-9033 (2022).
- 338 43 Good, S. N., Sharpe, R. J. & Johnson, J. S. Highly Functionalized Tricyclic Oxazinanones via
339 Pairwise Oxidative Dearomatization and N-Hydroxycarbamate Dehydrogenation: Molecular
340 Diversity Inspired by Tetrodotoxin. *J. Am. Chem. Soc.* **139**, 12422-12425 (2017).
- 341 44 Robins, J. G. & Johnson, J. S. An Oxidative Dearomatization Approach to Tetrodotoxin via a
342 Masked ortho-Benzoquinone. *Org. Lett.* **24**, 559-563 (2022).
- 343 45 Cho, Y. S., Carcache, D. A., Tian, Y., Li, Y.-M. & Danishefsky, S. J. Total Synthesis of (±)-
344 Jiadifenin, a Non-peptidyl Neurotrophic Modulator. *J. Am. Chem. Soc.* **126**, 14358-14359
345 (2004).
- 346 46 Xu, J., Trzoss, L., Chang, W. K. & Theodorakis, E. A. Enantioselective Total Synthesis of (–)-
347 Jiadifenolide. *Angew. Chem., Int. Ed.* **50**, 3672-3676 (2011).
- 348 47 Yang, Y., Fu, X., Chen, J. & Zhai, H. Total Synthesis of (–)-Jiadifenin. *Angew. Chem., Int. Ed.*
349 **51**, 9825-9828 (2012).
- 350 48 Yuan, C., Jin, Y., Wilde, N. C. & Baran, P. S. Short, Enantioselective Total Synthesis of Highly
351 Oxidized Taxanes. *Angew. Chem., Int. Ed.* **55**, 8280-8284 (2016).
- 352 49 Ohtawa, M. *et al.* Synthesis of (–)-11-O-Debenzoyletashironin: Neurotrophic Sesquiterpenes
353 Cause Hyperexcitation. *J. Am. Chem. Soc.* **139**, 9637-9644 (2017).
- 354 50 Condakes, M. L., Hung, K., Harwood, S. J. & Maimone, T. J. Total Syntheses of (–)-Majucin
355 and (–)-Jiadifenoxolane A, Complex Majucin-Type Illicium Sesquiterpenes. *J. Am. Chem. Soc.*
356 **139**, 17783-17786 (2017).
- 357 51 Leung, J. C. *et al.* Total Synthesis of (±)-Phomoidride D. *Angew. Chem., Int. Ed.* **57**, 1991-1994
358 (2018).

- 359 52 Tomanik, M., Xu, Z. & Herzon, S. B. Enantioselective Synthesis of Euonyminol. *J. Am. Chem. Soc.* **143**, 699-704 (2021).
- 360
- 361 53 Wang, Y., Nagai, T., Watanabe, I., Hagiwara, K. & Inoue, M. Total Synthesis of Euonymine and Euonyminol Octaacetate. *J. Am. Chem. Soc.* **143**, 21037-21047 (2021).
- 362
- 363 54 Köbrich, G. & Werner, W. α -Chlorepoxyde, α -chloraldehyde und α -hydroxyaldehyde aus carbonylverbindungen und dichlormethylithium. *Tetrahedron Lett.* **10**, 2181-2183 (1969).
- 364
- 365 55 Ken-ichi, S., Yasuhiro, K., Yutaka, N. & Juji, Y. Synthesis of the functionalized cyclohexanecarbaldehyde derivative. A potential key compound for total synthesis of optically active tetrodotoxin. *Chemistry Letters* **20**, 1559-1562 (1991).
- 366
- 367
- 368 56 Theurillat-Moritz, V. & Vogel, P. T.-a. Synthesis of enantiomerically pure 7-oxabicyclo[2.2.1]hept-2-enes precursors in the preparation of taxol analogues. *Tetrahedron: Asymmetry* **7**, 3163-3168 (1996).
- 369
- 370
- 371 57 Guidi, A., Theurillat-Moritz, V. & Vogel, P. Enantiomerically pure Diels-Alder adducts of maleic anhydride to furfural acetals through thermodynamic control. Single crystal and molecular structure of (1*S*, 4*R*, 4'*S*, 5'*S*)-1-(4', 5'-dimethyldioxolan-2'-yl)-5, 6-dimethylidene-7-oxabicyclo [2.2. 1] hept-2-ene. *Tetrahedron: Asymmetry* **7**, 3153-3162 (1996).
- 372
- 373
- 374
- 375 58 Chen, Y., McDaid, P. & Deng, L. Asymmetric alcoholysis of cyclic anhydrides. *Chem. Rev.* **103**, 2965-2984 (2003).
- 376
- 377 59 VanRheenen, V., Kelly, R. C. & Cha, D. Y. An improved catalytic OsO₄ oxidation of olefins to *cis*-1,2-glycols using tertiary amine oxides as the oxidant. *Tetrahedron Lett.* **17**, 1973-1976 (1976).
- 378
- 379
- 380 60 Crich, D. & Quintero, L. Radical chemistry associated with the thiocarbonyl group. *Chem. Rev.* **89**, 1413-1432 (1989).
- 381
- 382 61 Saraiva, M. F., Couri, M. R. C., Le Hyaric, M. & de Almeida, M. V. The Barton ester free-radical reaction: a brief review of applications. *Tetrahedron* **65**, 3563-3572 (2009).
- 383
- 384 62 Song, H.-T. *et al.* Photocatalytic decarboxylative hydroxylation of carboxylic acids driven by visible light and using molecular oxygen. *Org. Lett.* **81**, 7250-7255 (2016).
- 385
- 386 63 Zheng, C. *et al.* Ru-Photoredox-Catalyzed Decarboxylative Oxygenation of Aliphatic Carboxylic Acids through N-(acyloxy)phthalimide. *Org. Lett.* **20**, 4824-4827 (2018).
- 387
- 388 64 CronjéGrové, J., Holzapfel, C. W. & Williams, D. B. G. Stereoselective SmI₂-mediated conversion of carbohydrates into cyclopentanols. *Tetrahedron Letters* **37**, 1305-1308 (1996).
- 389
- 390 65 Chiara, J. L., Martínez, S. & Bernabé, M. Cascade Reaction of 6-Deoxy-6-iodohexopyranosides Promoted by Samarium Diiodide: A New Ring Contraction of Carbohydrate Derivatives. *J. Org. Chem.* **61**, 6488-6489 (1996).
- 391
- 392
- 393 66 Szostak, M., Spain, M. & Procter, D. J. Electron transfer reduction of unactivated esters using SmI₂-H₂O. *Chem. Commun.* **47**, 10254-10256 (2011).
- 394
- 395 67 Kim, K. S. & Qian, L. Improved method for the preparation of guanidines. *Tetrahedron Lett.* **34**, 7677-7680 (1993).
- 396
- 397 68 Feng, J., Kasun, Z. A. & Krische, M. J. Enantioselective Alcohol C-H Functionalization for Polyketide Construction: Unlocking Redox-Economy and Site-Selectivity for Ideal Chemical Synthesis. *J. Am. Chem. Soc.* **138**, 5467-5478 (2016).
- 398
- 399
- 400 69 Qiu, F. Strategic efficiency — The new thrust for synthetic organic chemists. *Can J. Chem.* **86**, 903-906 (2008).
- 401
- 402 70 Chen, T. G. *et al.* Building C(sp₃)-rich complexity by combining cycloaddition and C-C cross-

403 coupling reactions. *Nature* **560**, 350-354 (2018).

404

405 **Acknowledgments**

406 This work was supported by the National Natural Science Foundation of China (21971018 and
407 82225041). The authors gratefully acknowledge the Beijing Municipal Government and Tsinghua
408 University for their financial support. We thank Prof. Joseph Ready and Prof. Uttam Tambar for their
409 scientific comments and thank Drs. Jianwei Bian, Bo Liu, Shuanhu Gao, and Weiqing Xie for crucial
410 suggestions.

411 **Author contributions**

412 X.Q. conceived the study; P.C., J.W., and X.Q. designed the synthetic route and prepared the
413 manuscript; P.C. and J.W. carried out most of the chemical synthesis and prepared the supplemental
414 information; P.C., J.W., Y.W., Y.S., and Q.W. analyzed the data; S.Z., X.C., and P.C. performed the
415 biological study. All authors discussed the results and commented on the manuscript.

416 **Competing interest declaration**

417 The authors (Peihao Chen, Jing Wang, Yan Wang, Yuze Sun, Qingcui Wu, Xiangbing Qi) declare a
418 patent application based on this study (WIPO Application No. PCT/CN2022/111861).